HHS Public Access

Author manuscript

Chem Commun (Camb). Author manuscript; available in PMC 2016 May 28.

Published in final edited form as:

Chem Commun (Camb). 2015 May 28; 51(43): 8982–8985. doi:10.1039/c5cc01826a.

Cucurbit[6]uril is an ultrasensitive ^{129}Xe NMR contrast agent

Yanfei Wang[a] and **Ivan J. Dmochowski**[*,a]

[a] Department of Chemistry, University of Pennsylvania, Philadelphia, Pennsylvania 19104, USA

Abstract

A lack of molecular contrast agents has slowed the application of ultrasensitive hyperpolarized ^{129}Xe NMR methods. Here, we report that commercially available cucurbit[6]uril (CB[6]) undergoes rapid xenon exchange kinetics at 300 K, and is detectable by Hyper-CEST NMR at 1.8 pM in PBS and at 1 μM in human plasma where many molecules, including polyamines, can compete with xenon for CB[6] binding.

Hyperpolarized (HP) ^{129}Xe is being investigated for many NMR spectroscopy and imaging applications that require significant enhancements in detection sensitivity. The long-lived ^{129}Xe HP state is readily obtained by a process of spin-exchange optical pumping.[1] HP ^{129}Xe is non-toxic, can be delivered to living organisms via inhalation or Xe-solution injection,[2, 3] and has been employed for imaging the lungs and brain of living mammals, including human.[4-6] Xenon is very soluble in organic solvents and accumulates *in vivo* in lipid environments, while exhibiting low affinity for endogenous proteins and other biomolecules. Cryptophane-A and its derivatives (Scheme 1) are the most studied Xe-binding cages,[7, 8] and water-soluble versions exhibit association constants in excess of 30,000 M^{-1} at rt.[9-11] However, multi-step syntheses yield just milligram quantities of water-soluble cryptophane.[12] New xenon-binding contrast agents are needed to expand applications of HP ^{129}Xe in chemical sensing, biophysical chemistry, and biomedical imaging.

The unique hollow structures and molecular recognition properties of the cucurbit[n]uril (CB[n]) family have made CB[n] and functionalized CB[n] useful candidates as drug delivery vehicles, components of enzyme assays, and other sensing applications.[13, 14] Commercially available CB[6] (Scheme 1) possesses hexagonal symmetry with a hydrophobic cavity that is accessible through two carbonyl-fringed portals of ~4-Å diameter.[15, 16] CB[6] binds xenon with modest affinity but is poorly soluble in pure water. Interestingly, CB[6] becomes water soluble in the presence of monovalent cations (as found in biological fluids), however cation binding at the portals has been proposed to block xenon binding.[17] Here, we consider whether the CB[6] cavity, which is hydrophobic, rigidly open, and of similar dimensions to Xe (diameter ≈ 4.3 Å), can promote rapid Xe exchange interactions, as required for detection by HP ^{129}Xe chemical exchange saturation transfer (Hyper-CEST, Scheme 1).

* *ivandmo@sas.upenn.edu.*

† Electronic Supplementary Information (ESI) available: Materials, ITC data, 2D EXSY data, experimental parameters, and analysis of Hyper-CEST efficiency for samples with different putrescine concentrations. See DOI: 10.1039/b000000x/

Hyper-CEST NMR has recently enabled the ultrasensitive detection of cryptophanes,[18-25] gas-vesicle proteins,[26] and bacterial spores.[27] For example, our lab demonstrated 1.4 picomolar detection of a water-soluble tri-acetic acid cryptophane (TAAC, Scheme 1) at 320 K.[28] In Hyper-CEST, encapsulated HP ^{129}Xe is selectively depolarized by radiofrequency (rf) pulses, and the depolarized ^{129}Xe rapidly exchanges with HP ^{129}Xe to accumulate in the solvent pool, where loss of signal can be readily monitored. Stevens *et al.* reported a perfluorocarbon nanoemulsion contrast agent for ^{129}Xe NMR, with each droplet encapsulating multiple xenon atoms, depending on droplet size.[29] PFOB nanodroplets were recently applied for multiplexed detection using Hyper-CEST NMR in mammalian cells.[30] In order to advance many applications we have sought new molecular scaffolds for Hyper-CEST NMR. Here, the rapid, reversible complexation of xenon by CB[6] was investigated in physiologically relevant buffer solution (where CB[6] is soluble to greater than 10 mM), and exploited for Hyper-CEST NMR experiments in human plasma. Through selective saturation and magnetization transfer, the ^{129}Xe-CB[6] peak was encoded and amplified in the ^{129}Xe-solution peak (Scheme 1).

The HP ^{129}Xe NMR spectrum obtained with 5 mM CB[6] using a direct detection method showed that the ^{129}Xe-CB[6] peak in pH 7.2 PBS (1.058 mM potassium phosphate monobasic, 154 mM sodium chloride, and 5.6 mM sodium phosphate dibasic) was 72 ppm upfield-shifted from the ^{129}Xe-water peak (Figure 1). Due to rapid exchange of xenon with CB[6], the line shape of both ^{129}Xe NMR peaks appeared broad. Nonetheless, the "bound" ^{129}Xe peak was well-separated from the "free" peak, allowing it to be selectively irradiated with rf pulses without perturbing free HP ^{129}Xe in solution. Thermodynamic and kinetic parameters associated with the complexation of xenon by CB[6] at 300 K in PBS solution were determined by 2D HP ^{129}Xe NMR exchange spectroscopy (Figure S1). 2D-EXSY spectra were recorded with 2048 data points in t2 domain and 16 data points in t1 domain, using States-TPPI method in the t1 dimension. To evaluate the exchange rate constant, equations were used as described previously (Supporting Information).[31] The extracted rate constants for association and dissociation, k_{on} and k_{off}, were $4.1*10^5$ $M^{-1}s^{-1}$ and 840 s^{-1}, respectively. This result is similar to k_{off} values determined by Kim et al. for a more water-soluble CB[6] derivative: k_{off} = 2300 s^{-1} in water, k_{off} = 310 s^{-1} in 0.4 M Na^+ solution.[17] We determined the association constant ($K_A = k_{on}/k_{off}$) for xenon and CB[6] in PBS at pH 7.2 to be 490 M^{-1} at 300 K, in accord with previous measurements for this Xe-host interaction,[17, 32] taking into account the intermediate buffer salt concentration. The k_{off} value determined by EXSY was similar to the measured exchange rate from line-width analysis for the corresponding ^{129}Xe NMR spectrum (k_{exch} = 1470 s^{-1}, Figure S2). Xe affinity determined for CB[6] in PBS at 300 K was ~40-fold lower than measured previously for TAAC.[11] However, the ^{129}Xe-CB[6] exchange rate was ~17-fold higher than previously measured for ^{129}Xe-TAAC (k_{exch} = 86 s^{-1}) at 300 K,[28] and should afford efficient magnetization transfer, as required for ultrasensitive detection in the Hyper-CEST scheme.

To test CB[6] for Hyper-CEST NMR spectroscopy, multiple selective Dsnob-shaped saturation pulses were scanned over the chemical shift range of 85-210 ppm in 5-ppm steps. Two saturation responses were observed (Figure 2), centered at 193 ppm (^{129}Xe-aq) and 122 ppm (^{129}Xe-CB[6]). Similar to the direct detection spectrum with 5 mM CB[6] (Figure 1),

both peaks in the Hyper-CEST z-spectrum with 0.8 μM CB[6] appeared broad, which allowed for a broad saturation frequency window.

Ultrasensitive indirect detection of CB[6] was achieved by applying shaped rf saturation pulses at the chemical shift of ^{129}Xe in CB[6], and measuring the residual aqueous ^{129}Xe signal after spin transfer as on-resonance CEST response (Figure 3 and Figure S3). The observed depolarization response in Hyper-CEST experiments arose from both self-relaxation of HP ^{129}Xe and CB[6]-mediated saturation transfer. The depolarization rates were obtained by fitting both on-resonance and off-resonance decay curves to first-order exponential kinetics. Remarkably, 1.8 pM CB[6] was readily detected in PBS at 300 K (Figure 3). Average of three trials gave τ_{on} = 24.6 ± 1.2 s and τ_{off} = 58.5 ± 3.7 s. The high S/N at picomolar concentration is comparable to our previous Hyper-CEST measurements with TAAC, which required elevated temperature (320 K) to achieve similar 10^3 s^{-1} exchange kinetics.[28] As postulated previously for TAAC,[28] CB[6]-mediated exchange is likely enhanced by peripheral Xe atoms undergoing rapid magnetization transfer with the “bound” Xe atom at the primary site. Indeed, the open, tubular structure of CB[6] may promote rapid ^{129}Xe(primary)-^{129}Xe(periphery) interactions at both portals. Importantly, xenon is very soluble (4.2 mM atm^{-1}) in water at 300 K,[34] and working near rt is convenient for many biochemical and cellular assays.

Having established CB[6] as an ultrasensitive ^{129}Xe NMR contrast agent in physiologic buffer solution, we investigated the feasibility of using this agent in biological fluids. We first performed Hyper-CEST NMR experiments with 1 μM CB[6] in blood plasma (purchased from Sigma), and observed a peak at the characteristic ^{129}Xe-CB[6] chemical shift, 122 ppm (Figure 4). As expected, the aqueous Xe peak was broader, based on the faster exchange of HP ^{129}Xe in plasma. The many components of blood plasma that can interact with CB[6] also contributed to the HP ^{129}Xe-CB[6] peak being less intense than observed in PBS. Polyamines, for example, are naturally occurring organic molecules found in all living organisms and are known to have high affinity for CB[6] relative to other small molecules.[35] Polyamines are present at millimolar concentrations inside living cells, with ~10 percent being free polyamines, and at micromolar concentrations in biological fluids.[36, 37] Putrescine is believed to be the most abundant polyamine in most biological fluids, and is strongly associated with cancer and chemotherapy.[38, 39] We confirmed by isothermal titration calorimetry (ITC) that putrescine has high affinity for CB[6] in PBS (K_A = 3.6*10^6 M^{-1} at 300 K, Figure S4). To investigate the effect of putrescine on CB[6]-mediated Hyper-CEST signal in this biological fluid, we added 10 μM putrescine to the 1 μM CB[6]-plasma solution. The ^{129}Xe-CB[6] Hyper-CEST signal at 122 ppm remained visible but was reduced as a result of less free CB[6] in the sample (Figure 4). These experiments suggest that it is feasible to use CB[6] as a sensitive *in vivo* ^{129}Xe contrast agent in environments where competing polyamines exceed CB[6] concentration by less than 10-fold.

To quantify how polyamines affect CB[6] Hyper-CEST efficiency, we carried out a set of experiments with putrescine in PBS, which has similar salt concentration to plasma but affords longer T_1 (~60 sec) of HP ^{129}Xe. Putrescine concentrations of 1 μM to 50 μM were investigated, as this is the relevant range in biological fluids.[37] For each putrescine sample, 1

μM CB[6] was added and incubated for 20 min at 300 K. Then, the same Hyper-CEST NMR method was used as shown in Figure 3, with slightly adjusted saturation pulse (see Supporting Information for details). Saturation transfer efficiency (*ST*),[27] which is proportional to MR image contrast, and free CB[6] concentration were calculated for each putrescine sample (Table 1, see Supporting Information for details). With increasing putrescine in solution, the amount of CB[6] available for Xe exchange decreased, and a correspondingly smaller *ST* contrast value was observed. This experiment further demonstrated that only small excess of CB[6] (e.g., 5 nM CB[6] in PBS) is needed to generate useful Hyper-CEST contrast at intermediate field strength ($B_{1,max}$ = 92 μT).

A corollary from this experiment is that CB[6] enables fast and sensitive detection of putrescine in solution, without need for polyamine derivatization, by correlating the difference between on- and off-resonance HP ^{129}Xe decay rates to putrescine concentration. (See Figures S5 and S6 for more details.) To date, efforts with Hyper-CEST have focused on targeting proteins,[21] lipids,[19] or metal ions[24] by attaching different recognition moieties to cryptophane. Here, through competing guest encapsulation and “turn off” sensing, CB[6] affords new capabilities in small-molecule detection.

Conclusions

We demonstrated that commercially available cucurbit[6]uril can serve as a Hyper-CEST ^{129}Xe NMR contrast agent, both in physiologic buffer solution and a model biological fluid (human plasma). 2D-EXSY experiments confirmed that xenon k_{exch} with CB[6] is rapid but does not approach the fast exchange limit on the ^{129}Xe NMR time scale, which allowed the use of broadband irradiation to achieve efficient saturation of the ^{129}Xe-CB[6] complex without affecting free HP ^{129}Xe in solution. Efficient saturation transfer enabled low picomolar detection of CB[6] at 300 K, which was equivalent to the previous single-site Hyper-CEST detection record achieved in our laboratory using water-soluble cryptophane TAAC at 320 K.[28] Our data suggest that for many applications in aqueous buffer solution near rt, CB[6] should provide superior Hyper-CEST signal to water-soluble cryptophanes. A variety of cucurbituril derivatives[40] and acyclic variants[41, 42] have been reported that highlight opportunities for cucurbituril functionalization, as will likely be required to target specific biomolecules in solution.

CB[6] is very soluble in biological fluids and may also prove useful as a MRI/MRS contrast agent for *in vivo* applications. This will depend on the circulation time and localization of CB[6] *in vivo*, among other factors. One potential limitation of using CB[6] as a ^{129}Xe MR contrast agent is the competition for available xenon binding sites from endogenous small molecules. Importantly, saturation transfer efficiency was found to be strongly correlated with free CB[6] concentration, which is useful for establishing conditions that are amenable to the Hyper-CEST approach, even when the nature of the competing species is not perfectly known. For example, we showed that Hyper-CEST contrast can be achieved for CB[6] in plasma, which contains many competing species including high-affinity polyamines. Finally, we determined that it is possible to exploit the promiscuity of CB[6] to estimate the concentration of a known small molecule (e.g., putrescine) that competes with xenon for the binding cavity. The ready availability and versatile host-guest chemistry of CB[6] opens

many *in vitro* as well as *in vivo* applications, employing direct detection of $^{HP\ 129}Xe$ or Hyper-CEST NMR. Following our work with cryptophanes,[25, 43-45] we aim to develop cucurbituril xenon biosensors that take advantage of the special Hyper-CEST capabilities of this contrast agent.

Supplementary Material

Refer to Web version on PubMed Central for supplementary material.

Acknowledgments

We gratefully acknowledge Drs. George Furst and Jun Gu for assistance with NMR spectroscopy. This research was supported by NIH R01-GM097478 and CDMRP-LCRP Concept Award #LC130824; GM097478-S1 supported purchase of 795-nm laser.

References

1. Walker TG, Happer W. Rev. Mod. Phys. 1997; 69:629–642.
2. Albert MS, Cates GD, Driehuys B, Happer W, Saam B, Springer CS Jr. Wishnia A. Nature. 1994; 370:199–201. [PubMed: 8028666]
3. Nikolaou P, Coffey AM, Walkup LL, Gust BM, Whiting N, Newton H, Barcus S, Muradyan I, Dabaghyan M, Moroz GD, Rosen MS, Patz S, Barlow MJ, Chekmenev EY, Goodson BM. Proc. Natl. Acad. Sci. U. S. A. 2013; 110:14150–14155. [PubMed: 23946420]
4. Venkatesh AK, Zhang AX, Mansour J, Kubatina L, Oh CH, Blasche G, Selim Unlu M, Balamore D, Jolesz FA, Goldberg BB, Albert MS. Magn. Reson. Imaging. 2003; 21:773–776. [PubMed: 14559342]
5. Ruppert K, Mata JF, Brookeman JR, Hagspiel KD, Mugler JP 3rd. Magn. Reson. Med. 2004; 51:676–687. [PubMed: 15065239]
6. Mugler JP 3rd, Altes TA. J. Magn. Reson. Imaging. 2013; 37:313–331. [PubMed: 23355432]
7. Brotin T, Dutasta JP. Chem. Rev. 2009; 109:88–130. [PubMed: 19086781]
8. Taratula O, Hill PA, Khan NS, Carroll PJ, Dmochowski IJ. Nat. Commun. 2010:1. [PubMed: 20975674]
9. Jacobson DR, Khan NS, Colle R, Fitzgerald R, Laureano-Perez L, Bai Y, Dmochowski IJ. Proc. Natl. Acad. Sci. U. S. A. 2011; 108:10969–10973. [PubMed: 21690357]
10. Fairchild RM, Joseph AI, Holman KT, Fogarty HA, Brotin T, Dutasta JP, Boutin C, Huber G, Berthault P. J. Am. Chem. Soc. 2010; 132:15505–15507. [PubMed: 20958059]
11. Hill PA, Wei Q, Eckenhoff RG, Dmochowski IJ. J. Am. Chem. Soc. 2007; 129:11662–11662.
12. Taratula O, Hill PA, Bai Y, Khan NS, Dmochowski IJ. Org. Lett. 2011; 13:1414–1417. [PubMed: 21332141]
13. Isaacs L. Chem. Commun. 2009:619–629.
14. Lagona J, Mukhopadhyay P, Chakrabarti S, Isaacs L. Angew. Chem. Int. Ed. 2005; 44:4844–4870.
15. Freeman WA, Mock WL, Shih NY. J. Am. Chem. Soc. 1981; 103:7367–7368.
16. Hoffmann R, Knoche W, Fenn C, Buschmann H-J. J. Chem. Soc., Faraday Trans. 1994; 90:1507–1511.
17. Kim BS, Ko YH, Kim Y, Lee HJ, Selvapalam N, Lee HC, Kim K. Chem. Commun. (Camb). 2008:2756–2758. [PubMed: 18688300]
18. Schröder L, Lowery TJ, Hilty C, Wemmer DE, Pines A. Science. 2006; 314:446–449. [PubMed: 17053143]
19. Sloniec J, Schnurr M, Witte C, Resch-Genger U, Schröder L, Hennig A. Chem. Eur. J. 2013; 19:3110–3118. [PubMed: 23319433]
20. Klippel S, Döpfert J, Jayapaul J, Kunth M, Rossella F, Schnurr M, Witte C, Freund C, Schröder L. Angew. Chem. Int. Edit. 2014; 53:493–496.

21. Rose HM, Witte C, Rossella F, Klippel S, Freund C, Schröder L. Proc. Natl. Acad. Sci. U. S. A. 2014; 111:11697–11702. [PubMed: 25071165]
22. Schnurr M, Sydow K, Rose HM, Dathe M, Schröder L. Advanced Healthcare Materials. 2015; 4:40–45. [PubMed: 24985966]
23. Stevens TK, Palaniappan KK, Ramirez RM, Francis MB, Wemmer DE, Pines A. Magn. Reson. Med. 2013; 69:1245–1252. [PubMed: 22791581]
24. Tassali N, Kotera N, Boutin C, Leonce E, Boulard Y, Rousseau B, Dubost E, Taran F, Brotin T, Dutasta JP, Berthault P. Anal. Chem. 2014; 86:1783–1788. [PubMed: 24432871]
25. Riggle BA, Wang Y, Dmochowski IJ. J. Am. Chem. Soc. 2015 in press.
26. Shapiro MG, Ramirez RM, Sperling LJ, Sun G, Sun J, Pines A, Schaffer DV, Bajaj VS. Nat. Chem. 2014; 6:629–634. [PubMed: 24950334]
27. Bai Y, Wang Y, Goulian M, Driks A, Dmochowski IJ. Chem. Sci. 2014; 5:3197–3203. [PubMed: 25089181]
28. Bai Y, Hill PA, Dmochowski IJ. Anal. Chem. 2012; 84:9935–9941. [PubMed: 23106513]
29. Stevens TK, Ramirez RM, Pines A. J. Am. Chem. Soc. 2013; 135:9576–9579. [PubMed: 23742228]
30. Klippel S, Freund C, Schröder L. Nano Lett. 2014; 14:5721–5726. [PubMed: 25247378]
31. Zolnai Z, Juranić N, Vikić-Topić D, Macura S. J. Chem. Inf. Comput. Sci. 2000; 40:611–621. [PubMed: 10850767]
32. El Haouaj M, Luhmer M, Ko YH, Kim K, Bartik K. J. Chem. Soc. Perk. Trans. 2001; 2:804–807.
33. Zaiss M, Schnurr M, Bachert P. J. Chem. Phys. 2012; 136:144106. [PubMed: 22502500]
34. Clever, HL. Krypton, Xenon, and Radon: Gas Solubilities. Pergamon Press; Oxford: 1979.
35. Buschmann HJ, Mutihac L, Schollmeyer E. J. Incl. Phenom. Macrocycl. Chem. 2005; 53:85–88.
36. Thomas* T, Thomas TJ. CMLS, Cell. Mol. Life Sci. 2001; 58:244–258. [PubMed: 11289306]
37. Russell DH, Russell SD. Clin. Chem. 1975; 21:860–863. [PubMed: 48436]
38. Uriel Bachrach, YMH. The Physiology of Polyamines. CRC Press, Inc; 1989.
39. Gaboriau F, Havouis R, Moulinoux J-P, Delcros J-G. Anal. Biochem. 2003; 318:212–220. [PubMed: 12814624]
40. Kim K, Selvapalam N, Ko YH, Park KM, Kim D, Kim J. Chem. Soc. Rev. 2007; 36:267–279. [PubMed: 17264929]
41. Zhang B, Isaacs L. J. Med. Chem. 2014; 57:9554–9563. [PubMed: 25369565]
42. Minami T, Esipenko NA, Zhang B, Kozelkova ME, Isaacs L, Nishiyabu R, Kubo Y, Anzenbacher P. J. Am. Chem. Soc. 2012; 134:20021–20024. [PubMed: 23194337]
43. Chambers JM, Hill PA, Aaron JA, Han ZH, Christianson DW, Kuzma NN, Dmochowski IJ. J. Am. Chem. Soc. 2009; 131:563–569. [PubMed: 19140795]
44. Seward GK, Bai Y, Khan NS, Dmochowski I. Chem. Sci. 2011; 2:1103–1110. [PubMed: 25364495]
45. Wei Q, Seward GK, Hill PA, Patton B, Dimitrov IE, Kuzma NN, Dmochowski IJ. J. Am. Chem. Soc. 2006; 128:13274–13283. [PubMed: 17017809]

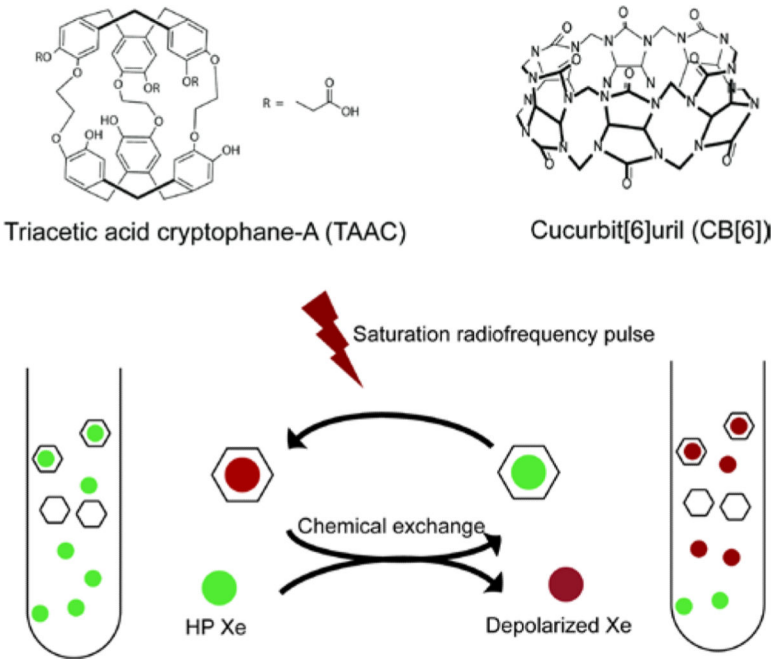

Scheme 1.

Top: Chemical structures of CB[6] and TAAC. Bottom: Hyper-CEST mechanism involving xenon-binding molecules represented by hexagons.

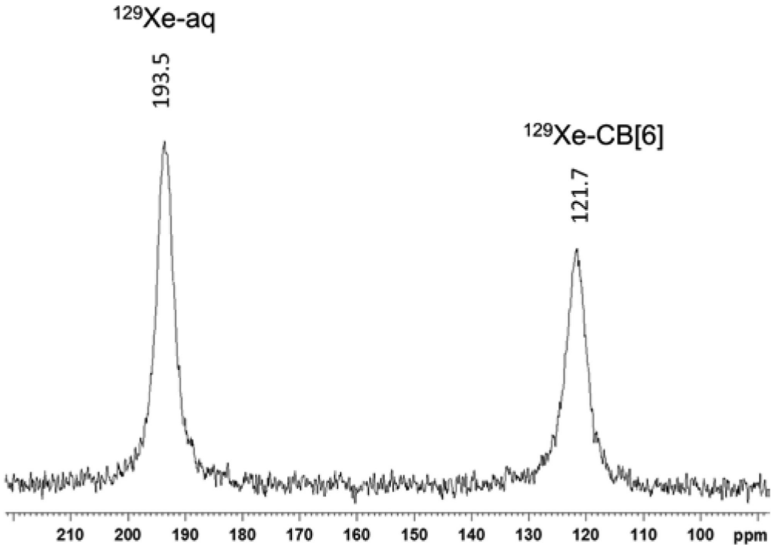

Figure 1.

HP ^{129}Xe NMR spectrum with 5 mM CB[6] dissolved in pH 7.2 PBS at 300 K. A 30 degree pulse was used and signal averaged over 8 scans. Fourier-transformed spectra were processed with zero-filling and Lorentzian line-broadening of 20 Hz. Peak width (FWHM) was 463 Hz for ^{129}Xe-aq peak, and 570 Hz for ^{129}Xe-CB[6] peak.

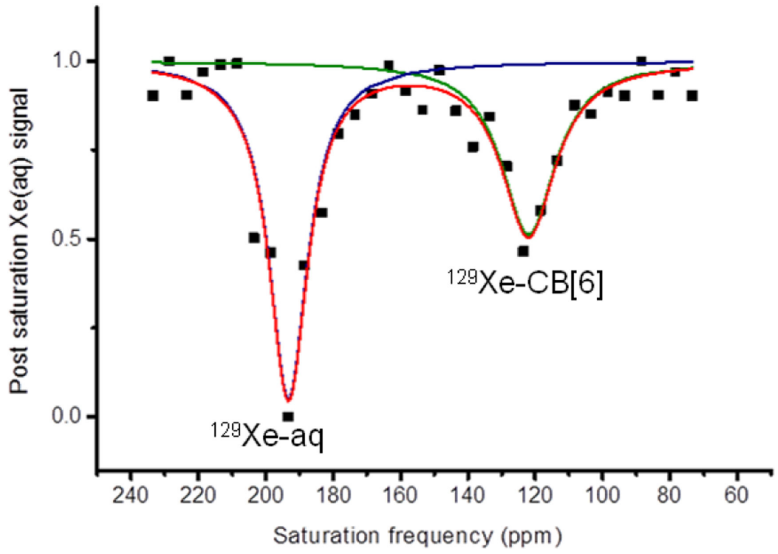

Figure 2.

Hyper-CEST frequency-scan profile of 0.8 μM CB[6] in pH 7.2 PBS at 300 K. When saturation rf pulse was positioned at 121 ppm (-72 ppm from ^{129}Xe-aq peak), encapsulated ^{129}Xe was depolarized and exchange caused rapid decrease in ^{129}Xe-aq signal. The black squares show the experimental data, and the lines show the exponential Lorentzian fits.[33]

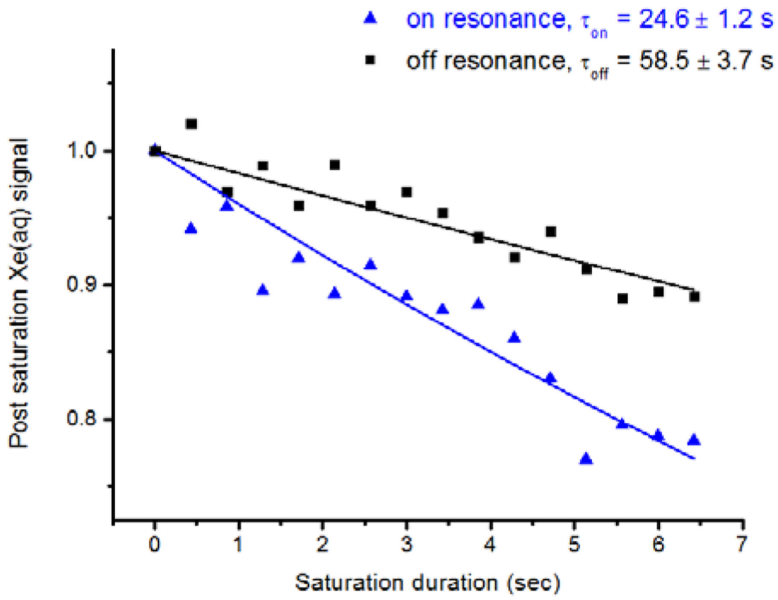

Figure 3.

Representative Hyper-CEST profile of 1.8 pM CB[6] in pH 7.2 PBS at 300 K. Saturation frequencies of Dsnob-shaped pulses were positioned at 122.3 ppm (193.5 – 71.2 ppm) and 264.7 ppm (193.5 + 71.2 ppm), for on- and off-resonance. Pulse length, τ_{pulse} = 1.05 ms; field strength, $B_{1,max}$ = 279 μT.

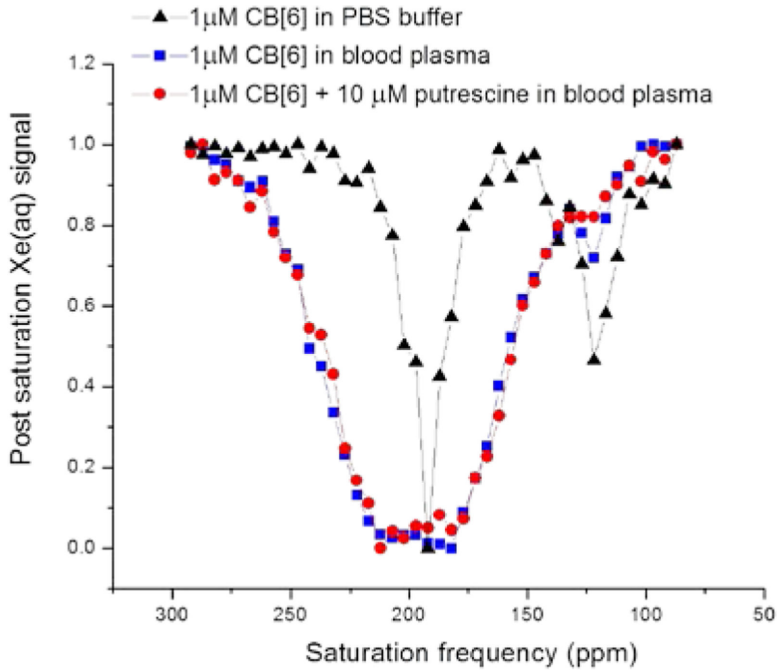

Figure 4.

Hyper-CEST spectra shown for 1 μM CB[6] in PBS (black), in blood plasma (blue), and in blood plasma with 10 μM putrescine (red); all data collected at 300 K.

Table 1

Saturation transfer *(ST)* efficiency for 1 μM CB[6] samples in PBS with varying putrescine concentration.

Putrescine (μM)	Calculated free CB[6] concentration (μM)	*ST* efficiency
0	1.0	0.68 ± 0.09
1	0.41	0.67 ± 0.10
2	0.19	0.34 ± 0.06
5	0.064	0.25 ± 0.03
10	0.030	0.16 ± 0.03
20	0.014	0.10 ± 0.01
50	0.0056	0.08 ± 0.01